Inorganic Chemistry

Article

pubs.acs.org/IC

Interaction of Insulin-Enhancing Vanadium Compounds with Human Serum holo-Transferrin

Daniele Sanna,[†] Giovanni Micera,[‡] and Eugenio Garribba*[,‡]

[†]Istituto CNR di Chimica Biomolecolare, Trav. La Crucca 3, I-07040 Sassari, Italy

[‡]Dipartimento di Chimica e Farmacia and Centro Interdisciplinare per lo Sviluppo della Ricerca Biotecnologica e per lo Studio della Biodiversità della Sardegna, Università di Sassari, Via Vienna 2, I-07100 Sassari, Italy

ABSTRACT: The interaction of VO^{2+} ion and four insulin-enhancing compounds, $[VO(ma)_2]$, $[VO(dhp)_2]$, $[VO(acac)_2]$, and *cis*-$[VO(pic)_2(H_2O)]$, where Hma, Hdhp, Hacac, and Hpic are maltol, 1,2-dimethyl-3-hydroxy-4(1*H*)-pyridinone, acetylacetone, and picolinic acid, with holo-transferrin (holo-hTf) was studied through the combined application of electron paramagnetic resonance (EPR) and density functional theory (DFT) methods. Since in holo-hTf all of the specific binding sites of transferrin are saturated by Fe^{3+} ions, VO^{2+} can interact with surface sites (here named sites C), probably via the coordination of His-N, Asp-COO^-, and Glu-COO^- donors. In the ternary systems with the insulin-enhancing compounds, mixed species are observed with Hma, Hdhp, and Hpic with the formation of VOL_2(holo-hTf), explained through the interaction of *cis*-$[VOL_2(H_2O)]$ (L = ma, dhp) or *cis*-$[VOL_2(OH)]^-$ (L = pic) with an accessible His residue that replaces the monodentate H_2O or OH^- ligand. The residues of His-289, His-349, His-473, and His-606 seem the most probable candidates for the complexation of the *cis*-VOL_2 moiety. The lack of a ternary complex with Hacac was attributed to the square-pyramidal structure of $[VO(acac)_2]$, which does not possess equatorial sites that can be replaced by the surface His-N. Since holo-transferrin is recognized by the transferrin receptor, the formation of ternary complexes between VO^{2+} ion, a ligand L^-, and holo-hTf may be a way to transport vanadium compounds inside the cells.

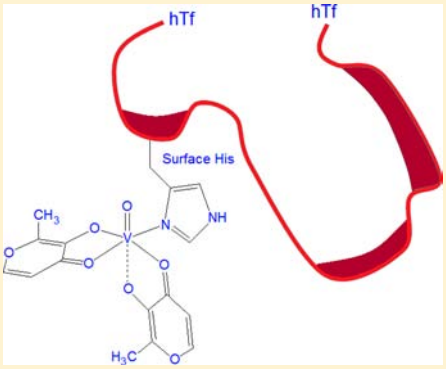

INTRODUCTION

Human serum transferrin is a single-chain glycoprotein containing 679 amino acids (~79 kDa) divided into two globular lobes that share 40% identity and 50% similarity.[1] These lobes are designated as N-terminal with some 330 residues (hTf_N) and C-terminal with some 340 residues (hTf_C) and are further composed of two subdomains (N1, residues 1−92 and 247−331; N2, residues 93−246; C1, residues 339−425 and 573−679; C2, residues 426−572 (hTf numbering)), which form a deep binding cleft.[1] The two lobes are connected by a short peptide linker (residues 332−338), which is a random coil in human serum transferrin but a three-turn helix in lactoferrin.

The main function of hTf is the transport of iron in the organism.[2] It binds reversibly two Fe^{3+} ions in the two sites in the N- and C-terminal regions: each Fe^{3+} ion is bound in a octahedral environment to Asp-63 from N1 (Asp-392 from C1), Tyr-95 from the edge of the N2 subdomain (Tyr-426 from the edge of the C2), Tyr-188 from N2 (Tyr-517 from C2), His-249 from hinge bordering N1 (His-585 from hinge bordering C1), and two oxygen atoms from the synergistic carbonate anion which is anchored in place by Arg-124 from N2 (Arg-456 from C2).[2−5] The binding of Fe^{3+} and carbonate causes the change of conformation from "wide-open" to "closed" form.[3,4,6] This involves a rotation of the N2 relative to the N1 domain of approximately 50° (53° for human lactoferrin[6]). Only the closed form of transferrin can be recognized by the hTf receptor, and it is internalized by the cell through a process known as receptor-mediated endocytosis.[2]

Depending on the saturation degree, hTf is indicated as apo-hTf (no iron bound), monoferric hTf (Fe-hTf_C or Fe-hTf_N), and diferric hTf (Fe_2-hTf). The iron-saturated protein is designated as holo-hTf. In normal plasma, only 30% of transferrin binds Fe^{3+} ions with a distribution of approximately 27% Fe_2-hTf, 23% Fe-hTf_N, 11% Fe-hTf_C, and 40% apo-hTf.[7] This corresponds to a concentration of ca. 50 μM of available binding sites. Therefore, transferrin can also bind other metal ions, including Bi^{3+}, Ga^{3+}, In^{3+}, Al^{3+}, Cu^{2+}, Mn^{2+}, Zn^{2+}, Ni^{2+}, Ru^{3+}, and vanadium in its three oxidation states (+3, +4, and +5).[3,4,8,9]

Strong evidence in the literature indicates that most of the vanadium in the serum is bound to hTf rather than albumin and IgG.[9−14] Concerning the biologically relevant oxidation states of V, they are +4 and +5, with +3 being very susceptible to oxidation.[9] It has been supposed that vanadium is transported in the blood, almost independently of its initial chemical form, as oxidovanadium(IV) or VO^{2+}.[13a,15]

The system VO^{2+}-hTf has been extensively studied through a wide variety of techniques. Electron paramagnetic resonance

Received: July 4, 2013
Published: October 3, 2013

   dx.doi.org/10.1021/ic401716x | *Inorg. Chem.* 2013, 52, 11975−11985

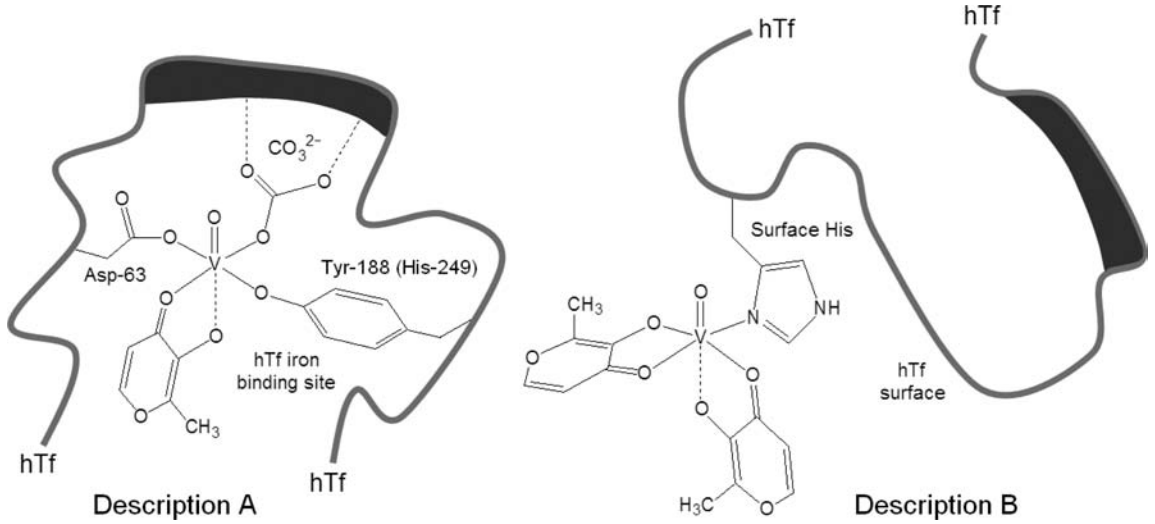

Figure 1. Proposed structures for the interaction of a VO^{2+} insulin-enhancing compound ($[VO(ma)_2]$ was taken as an example) with apo-hTf. On the left (VO)(apo-hTf)(L) (description A), suggested by Kiss and Costa Pessoa's groups (see refs 13b,c, 31, and 32). In this structure the moiety VOL^+ binds to the iron binding sites and the ligand L^- replaces two of the four coordinated amino acid residues. On the right *cis*-VOL_2(hTf) (description B), suggested by our research group (see refs 14c,d,f,g and 30). In this structure the moiety *cis*-$[VOL_2]$ interacts with an accessible His residue exposed on the protein surface. In both cases, the VO^{2+} binding to the protein is stabilized by a network of hydrogen bonds (not shown for clarity).

Scheme 1. Structure of the Four Insulin-Enhancing VO^{2+} Complexes Studied in This Work at the Physiological Conditions[a]

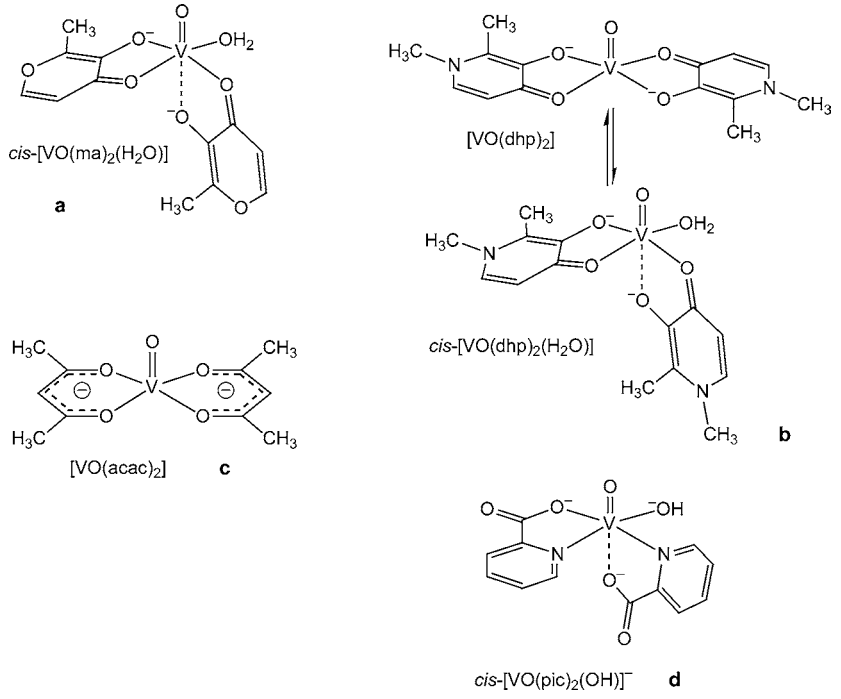

[a] The two forms $[VO(dhp)_2]$ and *cis*-$[VO(dhp)_2(H_2O)]$ are in equilibrium between each other.

(EPR) spectroscopy suggested that the VO^{2+} ion binds to the same sites of Fe^{3+}, one in the N-lobe (hTf_N) and the second in the C-lobe (hTf_C) of the protein.[14a,16−18] The binding of VO^{2+} in the two sites seems to be slightly different, and one conformer A (corresponding to the binding to the C-terminal site) and two conformers B (distinguished as B_1 and B_2, corresponding to the binding to the N-terminal site) are observed. Analogously to Fe^{3+}, VO^{2+} needs carbonate for binding to hTf. Carbonate can be replaced by other anions, called synergistic, which favor the metal coordination.[19] On the basis of these data and UV difference spectra, Smith et al. proposed for VO^{2+} ion bound in the hTf_C and hTf_N sites, the same coordination environment of Fe^{3+}.[20] This was confirmed recently by computational methods.[21] As verified also with Fe^{3+}, despite the same set of ligands, there is experimental evidence that the N- and C-lobes are not equivalent for VO^{2+}.[22]

Binding of non-iron metal ions to transferrin has also a significant role in the transport and delivery of metal drugs.[4,5,9,23−26] Vanadium species have been demonstrated to have insulin-enhancing properties.[9,27] A class of very promising

dx.doi.org/10.1021/ic401716x | *Inorg. Chem.* 2013, 52, 11975−11985

compounds consists of neutral VO^{2+} complexes with bidentate anionic ligands called also organic carriers (VOL_2); among these species, bis(maltolato)oxidovanadium(IV) (or BMOV) became the benchmark compound for the new molecules with insulin-enhancing action,[27a,c,28] and its derivative bis-(ethylmaltolato)oxidovanadium(IV) (or BEOV) arrived to phase IIa of clinical trials.[29] In this case the carrier ligand can participate in the transport processes in the blood, mainly through the interaction of VOL_2 species with transferrin.[9,13b,c,14,30] Up to now, two alternative descriptions of such mixed complexes formed by VO^{2+}, carrier, and hTf prevail in the literature: (i) we proposed the formulation (VO)(hTf)(L) when the carrier is a synergistic anion[14c,d] and *cis*-VOL_2(hTf) when it is not a synergistic anion and the V complex is in the octahedral *cis*-[$VOL_2(H_2O)$] form at the physiological conditions,[14f,g,30] and no interaction when VOL_2 is a species with square-pyramidal geometry;[14c] (ii) Kiss and Costa Pessoa's groups suggest in all of the systems containing VOL_2 (L = maltolate, 1,2-dimethyl-3-hydroxy-4(1*H*)-pyridinonato, and, recently, picolinato, dipicolinate, and pyrimidinonate derivatives) and hTf the formation of (VO)(hTf)(L), $(VO)_2$(hTf)-(L), and $(VO)_2$(hTf)$(L)_2$ independently on the features of the carrier (synergistic or not) and geometry assumed by the insulin-enhancing complex in aqueous solution.[13b,c,31,32] In particular, as illustrated in Figure 1, the formation of *cis*-VOL_2(hTf) is explained with the replacement of the equatorial water molecule by an imidazole N of an accessible His residue (presumably on the protein surface, Figure 1b); on the contrary, (VO)(hTf)(L), $(VO)_2$(hTf)(L), and $(VO)_2$(hTf)$(L)_2$ should derive from (VO)(hTf) and $(VO)_2$(hTf) in hTf_N and hTf_C sites with the bidentate carrier L^- replacing a His-249 (in the hTf_N) or His-585 (in the hTf_C) and Tyr-95 (in the hTf_N) or Tyr-426 (in the hTf_C) to form hexa-coordinated ternary VO^{2+}complexes (Figure 1a).[13c] It must be noticed that the stoichiometry *cis*-VOL_2(protein), with the equatorial binding of a His-N, was proposed for the first time by Orvig and co-workers for albumin and, subsequently, confirmed in the literature by other groups.[12,14c,f,33]

Until now, most of the studies on the interaction between metal compounds and transferrin were carried out using apo-hTf, because it has an open form and the two binding sites are available for metal ion coordination. On the contrary, holo-hTf has been studied less than apo-hTf, since the iron sites are occupied and not accessible. In this Article, the interaction of VO^{2+} ion and V insulin-enhancing complexes ([$VO(ma)_2$], [$VO(dhp)_2$], [$VO(acac)_2$], and *cis*-[$VO(pic)_2(H_2O)$], with ma indicating maltolato; dhp, 1,2-dimethyl-3-hydroxy-4(1*H*)-pyridinonato; acac, acetilacetonato; and pic, picolinato, see Scheme 1) with holo-transferrin is described. The systems were studied through EPR spectroscopy and density functional theory (DFT) methods. The experiments were compared with those obtained with apo-hTf.

In the interpretation of the data several points must be considered. (i) In in vitro experiments it was recently observed that VO^{2+} is easily oxidized to vanadium(V) in the presence of Fe^{3+} in solution;[32] however, in the human organism this process can be neglected, at least in a first approximation, because the presence of reducing agents such as ascorbate, catecholamines, and cysteine plus the binding of VO^{2+} by bioligands stabilizes the +IV state and significantly prevents its oxidation.[34] In vivo blood circulation monitoring—electron paramagnetic resonance (BCM-EPR) experiments performed on rats showed that approximately 90% or more of vanadium administered as $VOSO_4$ is present in the VO^{2+} form in nearly all organs.[35] (ii) The experiments are sensitive to the experimental procedure used to prepare the samples (in particular, to the variations of pH), and this may in part explain the different results obtained in the literature.[13b,14c,d,f,31,32]

The results reported in this study may contribute to understanding how the insulin-enhancing V compounds interact with transferrin at the physiological conditions and how they are transported in the organism.

EXPERIMENTAL AND COMPUTATIONAL SECTION

(1). Chemicals. Water was deionized prior to use through the purification system Millipore Milli-Q Academic. VO^{2+} solutions were prepared from $VOSO_4{\cdot}3H_2O$ following literature methods. Human serum apo-transferrin (apo-hTf) and human serum holo-transferrin (holo-hTf) were obtained from Sigma (T4382 and T4132, respectively) as lyophilized powders with a molecular mass of 76–81 kDa. The solubility of holo-hTf and apo-hTf is 20 mg/mL, corresponding to ca. 2.5×10^{-4} M. The concentration of the protein solutions was estimated from their UV absorption (ε_{280} = 92 300 M^{-1} cm^{-1}).[36] The other compounds used, i.e., maltol (Hma), 1,2-dimethyl-3-hydroxy-4(1*H*)-pyridinone (Hdhp), acetylacetone (Hacac), picolinic acid (Hpic), 1-methylimidazole (1-MeIm), $NaHCO_3$, and 4-(2-hydroxyethyl)-1-piperazineethanesulfonic acid (HEPES) were of the highest grade available and were used as received.

(2). Preparation of the Solutions. The solutions were prepared by dissolving in ultrapure water $VOSO_4{\cdot}3H_2O$ and the carrier (Hpic, Hacac, Hdhp, and Hma) to obtain a VO^{2+} concentration in the range of 5.0×10^{-4} to 1×10^{-3} M and a metal to carrier molar ratio of 1/2. Argon was bubbled through the solutions to ensure the absence of oxygen and avoid the oxidation of VO^{2+} ion.

In the systems containing only VO^{2+} and holo-hTf (see Figures 3 and 4), $VOSO_4{\cdot}3H_2O$ was dissolved in ultrapure water and pH raised to ca. 4.0; then, HEPES and $NaHCO_3$ were added to have a final concentration of 1.0×10^{-1} M and 2.5×10^{-2} M. Holo-hTf was added at pH 4.0, 5.2, and 7.4. In all the cases, pH was brought to 7.4 with a diluted solution of NaOH and EPR spectra were immediately measured.

In the systems containing also the organic carriers (Hma, Hdhp, Hacac, and Hpic; see Figures 5–8), the pH of the solutions, initially acid, was raised to ca. pH 5.0–5.5 with a diluted solution of NaOH, and HEPES and $NaHCO_3$ were added (final concentrations of 1.0×10^{-1} M and 2.5×10^{-2} M, respectively). Subsequently, pH was brought to 7.4, holo-hTf was added, and EPR spectra were measured.

The model systems VO^{2+}/carrier and VO^{2+}/carrier/1-MeIm were studied previously,[14d,f] and the results were used in this study to demonstrate the binding of vanadium species to holo-hTf.

(3). EPR Spectroscopy. EPR anisotropic spectra were recorded with an X-band (9.4 GHz) Bruker EMX spectrometer equipped with a HP 53150A frequency counter at 120 K. Low-temperature spectra were measured to minimize the oxidation of VO^{2+} ion to vanadium(V), which otherwise would happen very quickly, with a half-time between 5 and 13 min at room temperature.[36] When the samples were transferred into the EPR tubes, the spectra were immediately measured. To increase the signal-to-noise ratio, signal averaging was used.[14a,c]

(4). DFT Calculations. The coordination environment of VO^{2+} ion bound to the holo-hTf surface was described by performing DFT simulations with Gaussian 09 (revision C.01) software,[37] using the hybrid exchange-correlation functional B3LYP[38] and the basis set 6-311g.[39] This choice ensures a good degree of accuracy in the prediction of the structures of first-row transition metal complexes,[40] and in particular of vanadium compounds.[41] The solvent (H_2O) effect was simulated within the framework of the polarizable continuum model (PCM).[42]

The environment of VO^{2+} ion in the metal sites on the protein surface was simulated using 1-methylimidazole for His-N (N_{His}) and

acetate for Glu-COO^- or Asp-COO^- (COO^-_{Glu} and COO^-_{Asp}) coordination.[43] The symbols $N_{His}(\parallel)$ and $N_{His}(\perp)$ indicate an imidazole aromatic ring of a histidine residue arranged parallel and perpendicular to the V═O bond, respectively.

The ^{51}V **A** tensor was calculated using the functional BHandHLYP (as incorporated in Gaussian) and the 6-311g(d,p) basis set with Gaussian 09,[37] according to the procedures published in the literature.[14a,17,34a−c,43,44] It must be taken into account that for a VO^{2+} species A_z is usually negative, but in the literature its absolute value is usually reported. At a first-order approximation, the ^{51}V hyperfine coupling tensor **A** has two contributions: the isotropic Fermi contact (A_{iso}) and the anisotropic or dipolar hyperfine interaction (A^D):[45] $\mathbf{A} = A_{iso}\mathbf{1} + A^D$, where **1** is the unit tensor. The values of the ^{51}V anisotropic hyperfine coupling constants along the *x*, *y*, and *z* axes are as follows: $A_x = A_{iso} + A^D_x$, $A_y = A_{iso} + A^D_y$, and $A_z = A_{iso} + A^D_z$. The theory background was described in detail in ref 44c. The percent deviation from the absolute experimental value, $|A_z|^{exptl}$, was calculated as follows: $100 \times [(|A_z|^{calcd} - |A_z|^{exptl})/|A_z|^{exptl}]$ (see Table 1).

The analysis of surface amino acids of apo-hTf and holo-hTf was carried out with the software Swiss-Pdb Viewer version 4.0.4.[46]

RESULTS AND DISCUSSION

(1). Binary Systems VO^{2+}/holo-hTf and VO^{2+}/apo-hTf.

Anisotropic EPR spectra recorded on the systems VO^{2+}/apo-hTf and VO^{2+}/holo-hTf at pH 7.4 are shown in Figures 3 and 4. The spectrum of the binary system VO^{2+}/apo-hTf, previously reported (see trace a of Figures 3 and 4),[14a] can be described by postulating the formation of the species (VO)(apo-hTf) and/or $(VO)_2$(apo-hTf), depending on the ratio VO^{2+}/apo-hTf, in which the oxidovanadium(IV) ion is bound to one or both of the Fe^{3+} coordination sites. On this statement, a general consensus exists in the literature.[12,14a,16−18,47] In his fundamental works on the interaction VO^{2+}/hTf, Chasteen named A the site hTf_C and B the site hTf_N.[16] In the case of holo-hTf, two Fe^{3+} ions are present in the iron sites and, therefore, vanadium can occupy them only if it is able to replace Fe^{3+}. It is known that the release of Fe^{3+} coordinated to transferrin is facilitated by a pH decrease, which physiologically takes places in the endosomes, after the internalization of holo-hTf in the cell.[2] Iron is released from the N-lobe of human serum transferrin around pH 5.7, whereas the C-lobe retains Fe^{3+} ion until pH 4.8,[2] due to the protonation of some basic residues (Lys-206 and Lys-296 in the N-lobe, and Lys-534, Arg-632 and Asp-634 in the C-lobe).

For all of the systems studied, EPR resonances in the region of 50−190 mT were recorded. In this range, Fe^{3+} shows its characteristic signal with a weak transition around 70 mT ($g \sim 9.5$) and a composite pattern around 150 mT ($g \sim 4.3$); in particular, the absorption in the $g \sim 4.3$ region is unique for iron-transferrin proteins and can be used to establish the coordination mode of Fe^{3+} to the two binding sites of hTf.[48] The spectrum of holo-hTf (no V added) at pH 7.4 is shown in trace a of Figure 2. Aisen et al. demonstrated that the binding to Fe^{3+} of small polydentate ligands can modify the EPR signals around $g \sim 4.3$;[49] therefore, this can be a criterion to prove if the coordination environment of iron undergoes some changes.

In the binary system VO^{2+}/holo-hTf, the obtained results depend on the experimental procedure used, in particular, on the pH value at which VO^{2+} and holo-transferrin are put in contact (see Preparation of the Solutions in the Experimental and Computational Section). When the protein is added to a solution containing vanadium with a pH of ca. 4.0 (Figure 3b), the Fe^{3+} ions bound to the hTf binding sites are released and VO^{2+} can occupy both the hTf_N and hTf_C sites. At these conditions, the ratio Fe^{3+}/VO^{2+} in the hTf binding sites

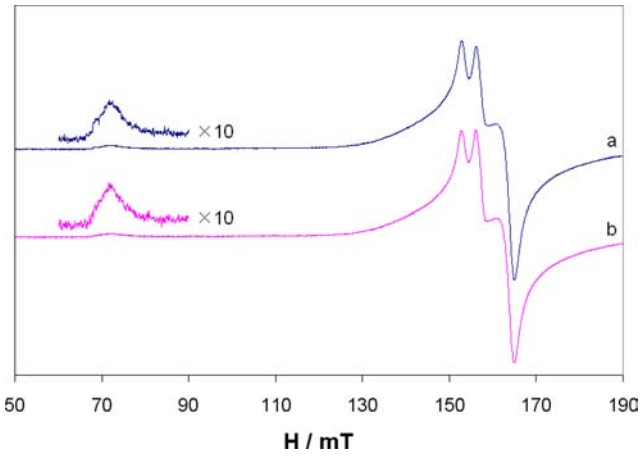

Figure 2. Iron signal region (50−190 mT) of the anisotropic X-band EPR spectra recorded at pH 7.4 on a frozen solution (120 K) containing (a) holo-hTf (2.5×10^{-4} M) and (b) 2/4/1 VO^{2+}/Hdhp/holo-hTf (holo-hTf, 2.5×10^{-4} M). The signals in the range of 60−90 mT were amplified 10 times.

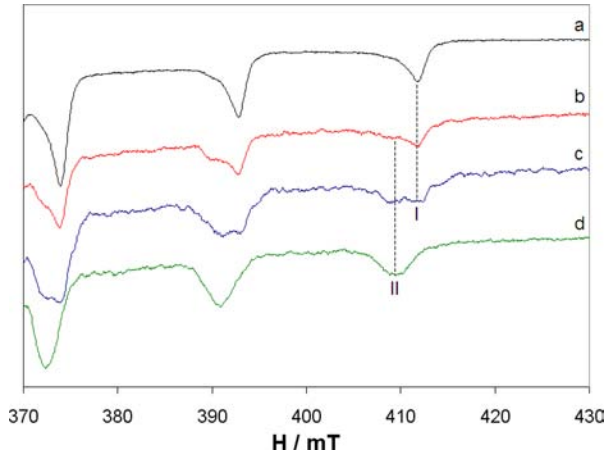

Figure 3. High-field region of the anisotropic X-band EPR spectra recorded at pH 7.4 on frozen solutions (120 K) containing (a) 2/1 VO^{2+}/apo-hTf (VO^{2+}, 5×10^{-4} M); (b) 2/1 VO^{2+}/holo-hTf (VO^{2+}, 5×10^{-4} M), in which holo-hTf was put in contact with VO^{2+} ion at pH ca. 4.0 and then pH raised to 7.4; (c) 2/1 VO^{2+}/holo-hTf (VO^{2+}, 5×10^{-4} M), in which holo-hTf was put in contact with VO^{2+} ion at pH 5.2 and then pH raised to 7.4; and (d) 2/1 VO^{2+}/holo-hTf (VO^{2+}, 5×10^{-4} M), in which holo-hTf was put in contact with VO^{2+} ion at pH 7.4. With the dotted lines are indicated the resonances $M_I = 7/2$ of the species in which the VO^{2+} ion is bound to the Fe specific sites (**I**) and to the nonspecific sites C (**II**), respectively.

depends on the ratio log K_1(Fe(hTf))/(log K_1(VO(hTf))): since log K_1(Fe(hTf)) > log K_1(VO(hTf)), a signal much weaker than that in the binary system VO^{2+}/apo-hTf is detected. However, for VO^{2+} an EPR spectrum similar to that recorded with apo-hTf is expected, i.e., with the same ratio between the signals of VO^{2+} ions in the two sites hTf_N and hTf_C (Figure 3a). The part of VO^{2+} not coordinated to the two binding sites remains in solution and can interact with nonspecific binding sites (we named these sites C): this is the reason for the appearance of the lower field resonances indicated by **II** in Figure 3. When holo-hTf is added at pH 5.2, Fe^{3+} is released mainly from hTf_N (see above) and most of VO^{2+} can interact with this site. With respect to the experiment at pH 4.0 a larger amount of vanadium remains in solution, and,

dx.doi.org/10.1021/ic401716x | Inorg. Chem. 2013, 52, 11975−11985

as a consequence, the relative concentration of the EPR signal bound to the nonspecific sites C increases. To prove these deductions, the low-field region of EPR spectra are reported in Figure 4. It can be observed that the intensity ratio between the

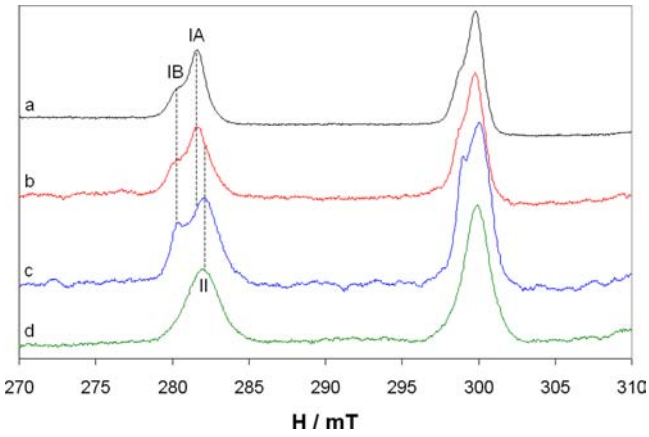

Figure 4. Low-field region of the anisotropic X-band EPR spectra recorded at pH 7.4 on frozen solutions (120 K) containing (a) 2/1 VO^{2+}/apo-hTf (VO^{2+}, 5×10^{-4} M); (b) 2/1 VO^{2+}/holo-hTf (VO^{2+}, 5×10^{-4} M), in which holo-hTf was put in contact with VO^{2+} ion at ca. pH 4.0 and then pH raised to 7.4; (c) 2/1 VO^{2+}/holo-hTf (VO^{2+}, 5×10^{-4} M), in which holo-hTf was put in contact with VO^{2+} ion at pH 5.2 and then pH raised to 7.4; (d) 2/1 VO^{2+}/holo-hTf (VO^{2+}, 5×10^{-4} M), in which holo-hTf was put in contact with VO^{2+} ion at pH 7.4. With the dotted lines are indicated the resonances $M_I = -7/2$ of the species in which the VO^{2+} ion is bound to the sites hTf_C (**IA**) and hTf_N (**IB**), and to the nonspecific sites C (**II**).

signals of hTf_N and hTf_C increases from the experiment at pH 4.0 (Figure 4b) to that at pH 5.2 (Figure 4c) because at this latter pH value most of the Fe^{3+} bound to hTf_C is not released. This also confirms that the resonances indicated with **IB** in Figure 4 belong to the hTf_N site.[16,36]

The binding to the nonspecific sites C is observed in an exclusive way when holo-hTf is put in contact with a VO^{2+} solution at pH 7.4 (trace d of Figures 3 and 4). EPR parameters are $g_z = 1.944$ and $A_z = 165.4 \times 10^{-4}$ cm^{-1} (Table 1), similar to those described for the species $(VO)_x$HSA.[12,14a,33,50] It is possible to advance some plausible hypotheses about the donor

Table 1. Possible Coordination Modes and ^{51}V Hyperfine Coupling Constant for the Site C of holo-hTf Obtained through DFT Simulations[a]

coordination[b]	A_x^{calcd}	A_y^{calcd}	A_z^{calcd}	A_z^{exptl}	dev[c]
$COO^-_{Glu/Asp}$, H_2O, H_2O, H_2O; H_2O^{ax}	−71.8	−70.3	−171.4	−165.4	3.6
N_{His}(∥), $COO^-_{Glu/Asp}$, H_2O, H_2O	**−68.0**	**−64.1**	**−167.8**	**−165.4**	**1.5**
N_{His}(∥), $COO^-_{Glu/Asp}$, $COO^-_{Glu/Asp}$, H_2O	−59.4	−57.0	−161.7	−165.4	−2.2
N_{His}(∥), N_{His}(⊥), $COO^-_{Glu/Asp}$, H_2O	**−64.2**	**−60.8**	**−164.9**	**−165.4**	**−0.3**
N_{His}(∥), N_{His}(∥), $COO^-_{Glu/Asp}$, H_2O	−60.2	−57.4	−162.0	−165.4	−2.1
N_{His}(∥), N_{His}(⊥), $COO^-_{Glu/Asp}$, $COO^-_{Glu/Asp}$	−55.8	−54.8	−158.9	−165.4	−3.9

[a]All values in 10^{-4} cm^{-1}. [b]In bold are indicated the more likely coordination modes. [c]Deviation from the experimental value calculated as $100 \times [(|A_z|^{calcd} - |A_z|^{exptl})/|A_z|^{exptl}]$.

atoms coordinated to vanadium by using DFT calculations on VO^{2+} model complexes. This approach consists of the comparison of the anisotropic hyperfine splitting constant of the ^{51}V nucleus (A_z) of a model species with that of a vanadium−protein and has been recently applied with excellent results to the study of the chemical environment of VO^{2+} ion in several biological systems.[43] In this work, this was used to describe the sites C of hTf. With the functional BHandHLYP and the basis set 6-311g(d,p) it is possible to calculate the A_z value for a VO^{2+} complex with an average deviation from the experimental value lower than 3%.[14a,44e] The optimization of the structure of the model complexes at the level of theory B3LYP/6-311g in water, simulating the effect of the solvent with the PCM, allows a further improvement of the estimated value of A_z.[43] The results of DFT calculations have been reported in Table 1. DFT simulations suggest that the binding sites C are nonspecific and involve the simultaneous coordination of accessible carboxylic groups belonging to aspartic and glutamic acid residues and imidazole groups of histidine residues. Of course, other possibilities may give an A_z value close to the experimental one; however, a coordination based on His-N and Asp/Glu-COO^- is in agreement with what was reported in the literature for the vanadium environment in carboxypeptidase ($A_z^{exptl} = 166 \times 10^{-4}$ cm^{-1} [51]), where—analogously to Zn^{2+}—the residues of Glu-72, His-69, and His-196 are coordinated to VO^{2+},[43,51] and the multimetal binding site of albumin ($A_z^{exptl} = 165-167 \times 10^{-4}$ cm^{-1}[14a,33]), where VO^{2+} ion is bound by His-67, His-247, and Asp-249.[33] The participation to the binding of stronger donor atoms such as Ser-O^- should give smaller values of A_z, as observed in VBrPO ($A_z^{exptl} = 160 \times 10^{-4}$ cm^{-1} [52,53]).

(2). Ternary Systems VO^{2+}/holo-hTf/maltol and VO^{2+}/apo-hTf/maltol. As demonstrated in the literature, the conformation of apo-hTf is open and the iron binding sites are exposed.[2−4,54] After the binding of Fe^{3+} and the synergistic anion carbonate to the holo-hTf, the conformation of the protein changes and the binding cleft results to be buried.[2−4,54]

In the binary system VO^{2+}/maltol with molar ratio 1/2, only the complex *cis*-$[VO(ma)_2(H_2O)]$ exists at pH 7.4 (**I** in Figure 5).[55] Anisotropic EPR spectra of the ternary system VO^{2+}/maltol/apo-transferrin were recorded with the two ratios 2/4/1 and 4/8/1 (traces e and f of Figure 5). Two species were detected (**IV** and **V** in Figure 5). One of them is the complex where VO^{2+} is bound to the Fe^{3+} sites of hTf ((VO)(apo-hTf) and/or $(VO)_2$(apo-hTf)), as it can be noticed by the comparison with the spectrum obtained in the binary system VO^{2+}/apo-hTf (**V** in traces e−g of Figure 5).[14a] The second species has been recently described in the literature as the ternary complex *cis*-VO$(ma)_2$(apo-hTf) (see Figure 1b) on the basis of the coincidence of the EPR resonances with those of *cis*-$[VO(ma)_2$(1-MeIm)] (1-methylimidazole can be considered a good model for the coordination of an imidazole His-N).[14f] In the same system, Kiss and Costa Pessoa groups have reported the formation of (VO)(apo-hTf)(ma), $(VO)_2$(apo-hTf)(ma), and $(VO)_2$(apo-hTf)$(ma)_2$, where the moiety $VO(ma)^+$ binds in the hTf_N and hTf_C sites with the bidentate carrier L^- replacing two of the four iron donors (Figure 1a).[13b,c,31] The formation of the two species **IV** and **V** is irrespective of the pH value at which apo-hTf is added to the solution containing *cis*-$[VO(ma)_2(H_2O)]$, pH 5.5 or 7.4; this is in agreement with the fact that the conformation of apo-hTf is open and, therefore, the two iron sites are accessible at the two pH values, and a part of vanadium, initially present as *cis*-$[VO(ma)_2(H_2O)]$, can be

dx.doi.org/10.1021/ic401716x | Inorg. Chem. 2013, 52, 11975−11985

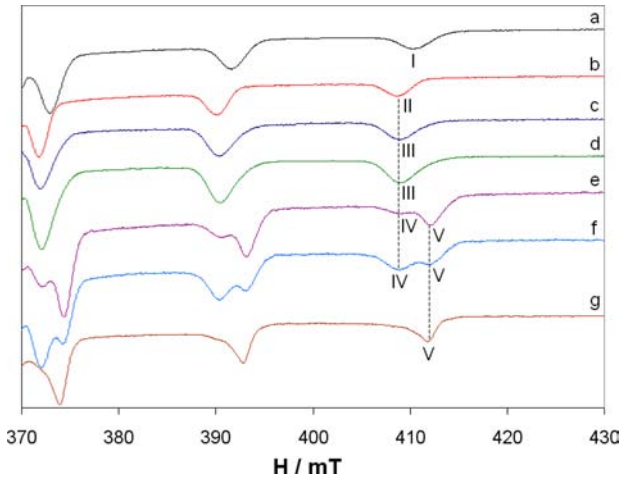

Figure 5. High-field region of the anisotropic X-band EPR spectra recorded at pH 7.4 on frozen solutions (120 K) containing: (a) 1/2 VO^{2+}/Hma (VO^{2+}, 1.0×10^{-3} M); (b) 1/2/5 VO^{2+}/Hma/1-MeIm (VO^{2+}, 1.0×10^{-3} M); (c) 2/4/1 VO^{2+}/Hma/holo-hTf (VO^{2+}, 5.0×10^{-4} M); (d) 4/8/1 VO^{2+}/Hma/holo-hTf (VO^{2+}, 1.0×10^{-3} M); (e) 2/4/1 VO^{2+}/Hma/apo-hTf (VO^{2+}, 5.0×10^{-4} M); (f) 4/8/1 VO^{2+}/Hma/apo-hTf (VO^{2+}, 1.0×10^{-3} M); and (g) 2/1 VO^{2+}/apo-hTf (VO^{2+}, 5.0×10^{-4} M). With the dotted lines are indicated the resonances $M_I = 7/2$ of the species *cis*-$[VO(ma)_2(1\text{-MeIm})]$ (**II**), *cis*-$VO(ma)_2$(apo-hTf) (**III**), *cis*-$VO(ma)_2$(holo-hTf) (**IV**), and (VO)(apo-hTf)/$(VO)_2$(apo-hTf) (**V**). With **I** is indicated the resonance $M_I = 7/2$ of *cis*-$[VO(ma)_2(H_2O)]$.

bound in such sites with the formation of the species (VO)(apo-hTf) and/or $(VO)_2$(apo-hTf). Another experimental observation that must be interpreted is the increase of the signal intensity of the mixed species **IV** at ratio 4/8/1 VO^{2+}/Hma/apo-hTf with respect to 2/4/1 (cf. traces e and f of Figure 5). This can be explained if the excess of *cis*-$[VO(ma)_2(H_2O)]$ binds to His surfaces forming a larger amount of *cis*-$VO(ma)_2$(apo-hTf). In other words, description B (Figure 1b) predicts that with a ratio of 4/8/1 part of vanadium is bound at the iron sites as (VO)(apo-hTf) and/or $(VO)_2$(apo-hTf), while the remaining part can only form mixed complexes with the involvement of surface His residues.

The examination of the system VO^{2+}/maltol/holo-transferrin with ratios 2/4/1 and 4/8/1 (traces c and d of Figure 5) provides further insights. In such a system the specific binding sites are occupied by Fe^{3+} and are inaccessible to the species *cis*-$[VO(ma)_2(H_2O)]$; therefore, the unique possibility is the formation of the mixed complex *cis*-$VO(ma)_2$(holo-hTf). On the basis of description B, EPR resonances should be coincident with those of *cis*-$[VO(ma)_2(1\text{-MeIm})]$ (**II** in trace b of Figure 5; $g_z = 1.948$ and $A_z = 164.8 \times 10^{-4}$ cm^{-1} [14f]), because only the surface histidines are accessible; this is experimentally observed, supporting the fact that holo-transferrin coordinates *cis*-$[VO(ma)_2(H_2O)]$ replacing the water molecule with a His-N. Interestingly, an increase of the ratio of VO^{2+} and maltol with respect to holo-hTf results in a significant increase of the spectral intensity of *cis*-$VO(ma)_2$(holo-hTf) because a greater amount of *cis*-$[VO(ma)_2(H_2O)]$ can be bound at the protein surface by accessible His residues. On the whole, the results obtained with holo-hTf confirm the formation of mixed species with composition *cis*-$VO(ma)_2$(apo-hTf) and *cis*-$VO(ma)_2$(holo-hTf), with the hTf bound to vanadium through His residues exposed on the protein surface. If vanadium binding was at the iron sites, we should expect different results in the case of apo- and holo-hTf; the only difference is, instead, the absence of the resonances of (VO)(apo-hTf) and/or $(VO)_2$(apo-hTf) with holo-transferrin (resonances indicated with **V** in traces e–g of Figure 5) because the specific sites are occupied by Fe^{3+} and inaccessible.

The distribution of the species after the interaction of the VO^{2+} complexes of maltol (but analogous conclusions are valid for the systems with Hdhp, Hacac, and Hpic; see below) with holo-transferrin demonstrates that when the insulin-enhancing compounds are added to the protein at pH 7.4, the iron sites are inaccessible because of the closed conformation. They may become available after the release of Fe^{3+}, which starts at pH < 5.7 for the protonation of Lys-206 and Lys-296 in the N-lobe.[2] On the contrary with apo-hTf, the open conformation is such that the iron binding sites (which are unoccupied) are exposed on the protein surface also at physiological pH too and, therefore, result in being accessible for the metal ion coordination.

(3). Ternary Systems VO^{2+}/holo-hTf/1,2-Dimethyl-3-hydroxy-4(1*H*)-pyridinone and VO^{2+}/apo-hTf/1,2-Dimethyl-3-hydroxy-4(1*H*)-pyridinone. In the ternary system VO^{2+}/apo-hTf/Hdhp (Figure 6d), previously described, the

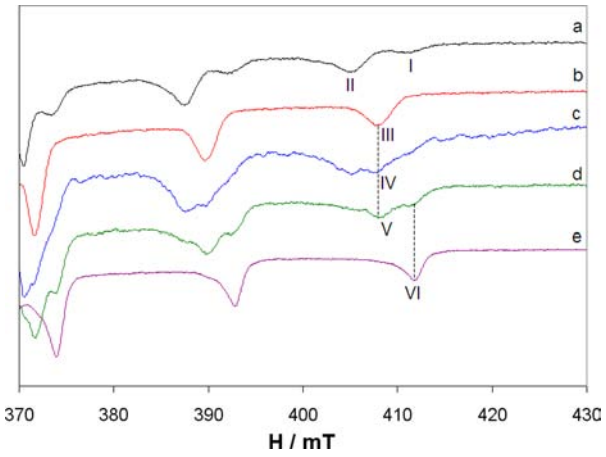

Figure 6. High-field region of the anisotropic X-band EPR spectra recorded at pH 7.4 on frozen solutions (120 K) containing (a) 1/2 VO^{2+}/Hdhp (VO^{2+}, 1×10^{-3} M); (b) 1/2/5 VO^{2+}/Hdhp/1-MeIm (VO^{2+}, 1×10^{-3} M); (c) 2/4/1 VO^{2+}/Hdhp/holo-hTf (VO^{2+}, 5×10^{-4} M); (d) 2/4/1 VO^{2+}/Hdhp/apo-hTf (VO^{2+}, 5×10^{-4} M); and (e) 2/1 VO^{2+}/apo-hTf (VO^{2+}, 5×10^{-4} M). With the dotted lines are indicated the resonances $M_I = 7/2$ of the species *cis*-$[VO(dhp)_2(1\text{-MeIm})]$ (**III**), *cis*-$VO(dhp)_2$(holo-hTf) (**IV**), *cis*-$VO(dhp)_2$(apo-hTf) (**V**), and (VO)(apo-hTf)/$(VO)_2$(apo-hTf) (**VI**). With **I** and **II** are indicated the resonances $M_I = 7/2$ of *cis*-$[VO(dhp)_2(H_2O)]$ and $[VO(dhp)_2]$.

following species are present at pH 7.4:[56] the binary complexes of Hdhp in the two isomeric forms *cis*-$[VO(dhp)_2(H_2O)]$ and $[VO(dhp)_2]$ (**I** and **II** in trace a of Figure 6), a small fraction of the binary species formed by apo-hTf, (VO)(apo-hTf) and/or $(VO)_2$(apo-hTf) (**VI** in trace e of Figure 6), and a mixed complex in which an imidazole nitrogen of a histidine residue of apo-hTf replaces the water molecule of *cis*-$[VO(dhp)_2(H_2O)]$ to form *cis*-$VO(dhp)_2$(apo-hTf) (see Scheme 2), whose coordination environment is analogous to *cis*-$[VO(dhp)_2(1\text{-MeIm})]$ formed in the ternary system VO^{2+}/Hdhp/1-methylimidazole (**III** in trace b of Figure 6).

In the case of the ternary system VO^{2+}/Hdhp/holo-hTf, the vanadium coordination at the iron sites is not possible, since

dx.doi.org/10.1021/ic401716x | *Inorg. Chem.* 2013, 52, 11975–11985

Scheme 2. Proposed Structures for the Mixed Complexes Formed by apo-hTf and holo-hTf with maltol and dhp: (a) *cis*-VO(ma)$_2$(apo-hTf) or *cis*-VO(ma)$_2$(holo-hTf) and (b) *cis*-VO(dhp)$_2$(apo-hTf) or *cis*-VO(dhp)$_2$(holo-hTf)

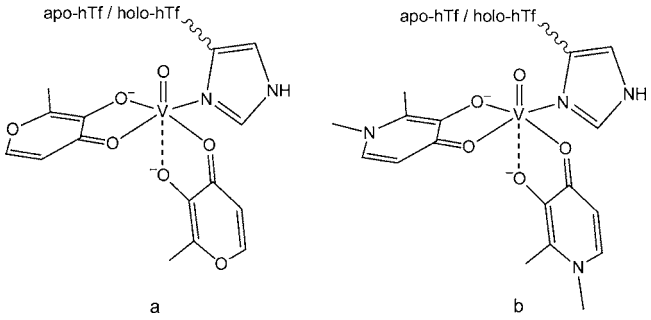

these are occupied by Fe^{3+} ion. The region with the iron signals (50−190 mT) is shown in trace b of Figure 2, where it is observable that the EPR resonances do not change with respect to the system with holo-hTf (cf. traces a and b of Figure 2), indicating that the two Fe^{3+} ions maintain their chemical environment. Therefore, vanadium distributes between the binary complexes of Hdhp and the mixed species *cis*-VO(dhp)$_2$(holo-hTf), identical to that previously described in the case of apo-hTf with the coordination of an imidazole nitrogen of a surface histidine residue on the equatorial plane of the VO^{2+} ion (**IV** in trace c of Figure 6). A comparison between the systems VO^{2+}/Hdhp/apo-hTf and VO^{2+}/Hdhp/holo-hTf (traces c and d of Figure 6) shows, however, two important differences: in the system with holo-hTf the resonances of the species (VO)(apo-hTf)/(VO)$_2$(apo-hTf) are not observed since the specific sites are occupied by the Fe^{3+} ion and the relative concentration of *cis*-VO(dhp)$_2$(holo-hTf) decreases with respect to *cis*-VO(dhp)$_2$(apo-hTf). This latter observation can be related to the decrease of the number of surface histidines when comparing apo- with holo-hTf. The analysis of surface His residues of apo-hTf and holo-hTf was carried out with the software Swiss-Pdb Viewer,[46] examining the structures indicated with 2HAU [57] and 3V83 [58] in the Protein Data Bank. Swiss-Pdb Viewer can be used to find the residues with an accessible surface area higher than a given percentage. Selecting 25% as a threshold value to consider an amino acid as fully accessible for metal coordination, apo-hTf has six histidine residues exposed on the surface (His-14, His-289, His-349, His-350, His-606, and His-642), whereas holo-hTf has only four residues (His-289, His-349, His-473, and His-606).

(4). Ternary Systems VO^{2+}/holo-hTf/Acetylacetone and VO^{2+}/apo-hTf/Acetylacetone. In the system VO^{2+}/apo-hTf/Hacac the species (VO)(apo-hTf)/(VO)$_2$(apo-hTf) (**I** in Figure 7) and [VO(acac)$_2$] (**II** in Figure 7) coexist. The absence of a mixed species VO−apo-hTf−acac was explained in terms of the geometry of the bis-chelated insulin-enhancing compound formed by acetylacetonate, square-pyramidal rather than *cis*-octahedral (see Scheme 1), which hinders the coordination of an accessible His residue on the equatorial plane of VO^{2+} ion.[14c] On the basis of these results, also the formation of (VO)$_2$(apo-hTf)(acac) and (VO)$_2$(apo-hTf)-(acac)$_2$, possible in principle due to the insertion of an acetylacetonate anion in the iron specific sites, can be excluded.

The different behavior of the system with holo-transferrin with respect to that with apo-transferrin confirms our conclusions. The ternary system VO^{2+}/Hacac/holo-hTf (Figure 7c) shows that vanadium, which cannot be transferred to the

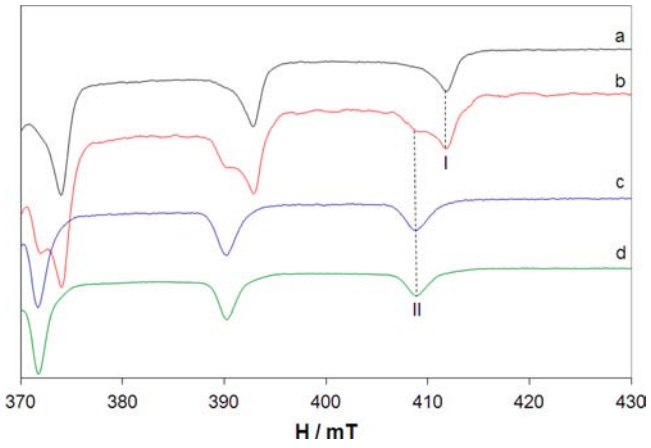

Figure 7. High-field region of the anisotropic X-band EPR spectra recorded at pH 7.4 on frozen solutions (120 K) containing (a) 2/1 VO^{2+}/apo-hTf (VO^{2+}, 5×10^{-4} M); (b) 2/4/1 VO^{2+}/Hacac/apo-hTf (VO^{2+}, 5×10^{-4} M); (c) 2/4/1 VO^{2+}/Hacac/holo-hTf (VO^{2+}, 5×10^{-4} M); and (d) 1/2 VO^{2+}/Hacac (VO^{2+}, 1×10^{-3} M). With the dotted lines are indicated the resonances M_I = 7/2 of the species (VO)(apo-hTf)/(VO)$_2$(apo-hTf) (**I**) and [VO(acac)$_2$] (**II**).

iron sites since these are occupied and inaccessible, is present in solution only as [VO(acac)$_2$]. In fact the bis-chelated complex with acetylacetonate, having a square-pyramidal coordination geometry (see Scheme 3a), does not have any tendency to form

Scheme 3. Structure of the Complex [VO(acac)$_2$] (a) and Proposed Structure of the Mixed Species Formed by holo-hTf with Picolinic Acid, *cis*-VO(pic)$_2$(holo-hTf) (b)

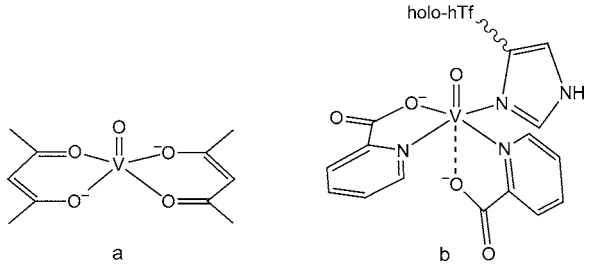

mixed complexes of the type *cis*-VO(carrier)$_2$(protein), differently from what was previously observed with Hma and Hdhp. The fact that no ternary species is formed by VO^{2+}, acetylacetonate, and 1-methylmidazole further supports these findings.[14c]

(5). Ternary Systems VO^{2+}/holo-hTf/Picolinic Acid and VO^{2+}/apo-hTf/Picolinic Acid. In the binary system VO^{2+}/picolinic acid with molar ratio 1/2, vanadium is present in solution at physiological pH mainly as the complex *cis*-[VO(pic)$_2$(OH)]$^-$ (**V** in trace e of Figure 8), while the bis-chelated *cis*-[VO(pic)$_2$(H$_2$O)] and the hydrolytic [(VO)$_2$(OH)$_5$]$^-$ species exist in smaller amounts; this was demonstrated by EPR and pH-potentiometric measurements.[59]

The ternary systems VO^{2+}/Hpic/apo-hTf and VO^{2+}/Hpic/holo-hTf show a very different behavior. In the system containing apo-hTf (Figure 8a), vanadium is bound to the iron sites to form (VO)(apo-hTf) and (VO)$_2$(apo-hTf) (**I** in Figure 8), which are in equilibrium with the mixed complex (VO)(apo-hTf)(pic) (**II** in Figure 8), in which picolinate ion, behaving as a synergistic anion, replaces bicarbonate in the specific sites. This type of coordination is indicated by the

dx.doi.org/10.1021/ic401716x | *Inorg. Chem.* 2013, 52, 11975−11985

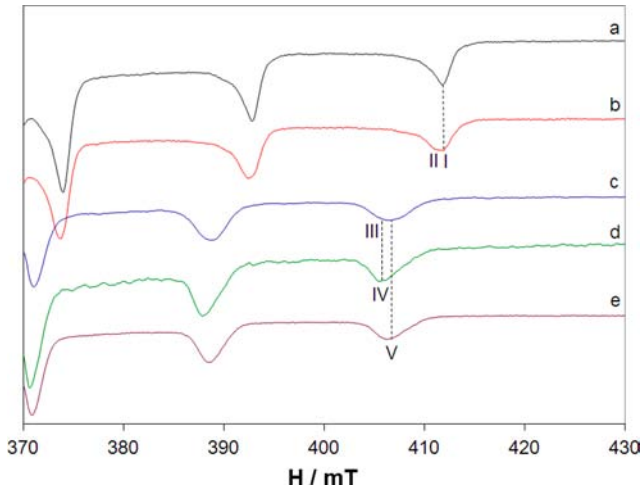

Figure 8. High-field region of the anisotropic X-band EPR spectra recorded at pH 7.4 on frozen solutions (120 K) containing (a) 2/1 VO^{2+}/apo-hTf (VO^{2+}, 5×10^{-4} M); (b) 2/4/1 VO^{2+}/Hpic/apo-hTf (VO^{2+}, 5×10^{-4} M); (c) 2/4/1 VO^{2+}/Hpic/holo-hTf (VO^{2+}, 5×10^{-4} M); (d) 1/2/5 VO^{2+}/Hpic/1-MeIm (VO^{2+}, 1×10^{-3} M); and (e) 1/2 VO^{2+}/Hpic (VO^{2+}, 1×10^{-3} M). With the dotted lines are indicated the resonances $M_I = 7/2$ of the species (VO)(apo-hTf)/$(VO)_2$(apo-hTf) (**I**), *cis*-$VO(pic)_2$(holo-hTf) (**III**), *cis*-$[VO(pic)_2(1\text{-MeIm})]$ (**IV**), and *cis*-$[VO(pic)_2(OH)]^-$ (**V**). With **II** are indicated the resonances $M_I = 7/2$ of the species (VO)(apo-hTf)(pic).

shoulder appearing at lower fields with respect to the resonance $M_I = 7/2$ of (VO)(apo-hTf)/$(VO)_2$(apo-hTf).[14c] It must be highlighted that, for apo-hTf, the EPR spectrum of the mixed species VO−apo-hTf−pic ($A_z \sim 167 \times 10^{-4}$ cm^{-1}) is significantly different from that of the complex *cis*-$[VO(pic)_2(1\text{-MeIm})]$ ($A_z = 158.8 \times 10^{-4}$ cm^{-1});[14c] this proves that the coordination environment is similar to that of VO^{2+} in the iron sites and that the formation of the species in which a His-N would replace the OH^- ion in the equatorial position, possible in principle, can be ruled out.

In the system containing holo-hTf (Figure 8c), there are no EPR transitions ascribable to VO^{2+} bound in the iron sites, and a large band in the magnetic field range of 403−410 mT appears, due to the superimposition of the $M_I = 7/2$ transitions of two different species. The position of the signals is comparable with that of the resonances of *cis*-$[VO(pic)_2(OH)]^-$ (**V** in trace e of Figure 8) and the mixed complex *cis*-$[VO(pic)_2(1\text{-MeIm})]$ (**IV** in trace d of Figure 8), whose existence in solution at pH 7.4 was confirmed by pH-potentiometry.[14d] This indicates that, in the system with holo-hTf, comparable amounts exist for both complexes *cis*-$[VO(pic)_2(OH)]^-$ and *cis*-$VO(pic)_2$(holo-hTf) (**III** in trace c of Figure 8), in which the coordination is [(N, COO^-); (N, COO^{-ax}); N_{His}] (see Table 2). At these conditions, the formation of a ternary complex in the iron sites (with hypothetical stoichiometry (VO)(holo-hTf)(pic)) is hindered by the presence of Fe^{3+} in those sites.

CONCLUSION

In this study the interaction between holo-transferrin and VO^{2+} ion and four insulin-enhancing compounds ($[VO(maltolato)_2]$, $[VO(1,2\text{-dimethyl-3-hydroxy-4(1}H\text{)-pyridinonato})_2]$, $[VO(acetylacetonato)_2]$, and *cis*-$[VO(picolinato)_2(H_2O)]$) is described. In the holo-transferrin all of the specific metal binding sites are occupied by Fe^{3+} and vanadium is forced to interact with other sites.

The results prove definitely that, in apo-hTf VO^{2+}, binds to the hTf_N and hTf_C sites. In holo-hTf, this possibility is precluded and VO^{2+} ions interact with never reported surface sites (named sites C), probably via the coordination of His-N, Asp-COO^-, and Glu-COO^- donors.

The data obtained with the insulin-enhancing compounds in the systems with holo-transferrin must be taken into account to establish which type of mixed complex is formed between VO^{2+}, apo-hTf (or holo-hTf), and the ligand L^-. As mentioned in the Introduction, two different descriptions are reported in the literature (descriptions A and B in Figure 1): description B predicts the formation of *cis*-VOL_2(apo-hTf) complexes with the equatorial coordination of a surface His-N when L^- is not a synergistic anion that stabilizes at the physiological conditions the *cis*-octahedral geometry,[14c,d,f,g,30] whereas the description A postulates the formation of (VO)(apo-hTf)(L), $(VO)_2$(apo-hTf)(L) and $(VO)_2$(apo-hTf)$(L)_2$ at the iron specific

Table 2. EPR Parameters of the Complexes Formed by VO^{2+} with apo- and holo-hTf

species	g_z	$A_z/(10^{-4}$ $cm^{-1})$	donors	ref
(VO)(apo-hTf_C)	1.937	168.3	Asp-392, Tyr-426, Tyr-517, His-585, CO_3^{2-}	14a
(VO)(apo-hTf_N)	1.941	170.5	Asp-63, Tyr-95, Tyr-188, His-249, CO_3^{2-}	14a
(VO)(apo-hTf_N)	1.935	171.8	Asp-63, Tyr-95, Tyr-188, His-249, CO_3^{2-}	14a
(VO)(holo-hTf)	1.944	165.4	sites C of hTf (see Table 1)	*a*
cis-$[VO(ma)_2(H_2O)]$	1.942	170.2	(CO, O^-); (CO, O^{-ax}); H_2O	14f
cis-$[VO(ma)_2(1\text{-MeIm})]$	1.948	164.8	(CO, O^-); (CO, O^{-ax}); N_{im}	14f
cis-$VO(ma)_2$(apo-hTf)	1.947	165.3	(CO, O^-); (CO, O^{-ax}); N_{His}	14f
cis-$VO(ma)_2$(holo-hTf)	1.946	165.4	(CO, O^-); (CO^{ax}, O^-); N_{His}	*a*
$[VO(acac)_2]$	1.948	166.4	(CO, O^-); (CO, O^-)	14c
$[VO(dhp)_2]$	1.951	158.3	(CO, O^-); (CO, O^-)	14c
cis-$[VO(dhp)_2(H_2O)]$	1.940	166.1	(CO, O^-); (CO, O^{-ax}); H_2O)	14c
cis-$[VO(dhp)_2(1\text{-MeIm})]$	1.947	163.0	(CO, O^-); (CO, O^{-ax}); N_{im}	14c
cis-$VO(dhp)_2$(apo-hTf)	1.947	163.3	(CO, O^-); (CO^{ax}, O^-); N_{His}	14c
cis-$VO(dhp)_2$(holo-hTf)	1.947 [b]	~163 [b]	(CO, O^-); (CO^{ax}, O^-); N_{His}	*a*
cis-$[VO(pic)_2(OH)]^-$	1.947	159.8	(N, COO^-); (N, COO^{-ax}); OH^-	14c
cis-$[VO(pic)_2(1\text{-MeIm})]$	1.943	158.8	(N, COO^-); (N, COO^{-ax}); N_{im}	14c
cis-$VO(pic)_2$(holo-hTf)	1.949	161.0	(N, COO^-); (N, COO^{-ax}); N_{His}	*a*

[a]This work. [b]Values measurable only approximately because of the presence of more than one species.

dx.doi.org/10.1021/ic401716x | *Inorg. Chem.* 2013, 52, 11975−11985

sites.[13b,c,31,32] In the systems with holo-hTf, these species should not be observed because the specific sites are occupied by Fe^{3+}. Instead, the same resonances detected with apo-hTf—and interpreted as *cis*-VOL_2(apo-hTf)—are experimentally observed with maltolate, dhp and picolinate; this means that the same species *cis*-VOL_2(holo-hTf) should be formed with the coordination of an exposed donor of the polypeptide chain. The system with picolinic acid appears to be particularly interesting: with apo-hTf, it forms (VO)(apo-hTf)(pic) because the iron sites are free and picolinate ligand behaves as a synergistic anion, whereas with holo-hTf it gives *cis*-$VO(pic)_2$(holo-hTf) because the sites are blocked by Fe^{3+} ions; it is noteworthy that the two mixed species (VO)(apo-hTf)(pic) and *cis*-$VO(pic)_2$(holo-hTf) are characterized by two significantly different values of ^{51}V A_z (see traces b and c of Figure 8). On the basis of this experimental evidence, we explain the formation of *cis*-VOL_2(apo-hTf) or *cis*-VOL_2(holo-hTf) through the interaction of *cis*-$[VOL_2(H_2O)]$ or *cis*-$[VOL_2(OH)]^-$ with the accessible (presumably, on the protein surface) His residues give a complex *cis*-VOL_2(holo-hTf) analogous to that proposed for apo-hTf (indeed, the ^{51}V A_z value is the same). The residues of His-289, His-349, His-473, and His-606 for holo-hTf and His-14, His-289, His-349, His-350, His-606, and His-642 for apo-hTf seem the most probable candidates for the complexation of the *cis*-VOL_2 moiety. Only with acetylacetonate, ternary compounds cannot be formed because $[VO(acac)_2]$ does not possess equatorial sites that can be easily replaced by the surface His-N.

Here we'd like to highlight that these conclusions are based mainly on EPR spectroscopy and that other evidence (for example, an X-ray diffraction analysis) is necessary to establish if both of the two descriptions (description A which postulates the existence of (VO)(apo-hTf)(L), $(VO)_2$(apo-hTf)(L), and $(VO)_2$(apo-hTf)$(L)_2$ and description B which postulates the formation of *cis*-VOL_2(apo-hTf) or *cis*-VOL_2(holo-hTf)) or only one of them is correct; it must be noticed that, in these systems, the results of the experiments are strongly dependent on the conditions used and these may favor the formation of different species. It is probable that the use of only spectroscopic techniques (EPR, CD, and UV−vis spectroscopy) would not permit one to demonstrate unequivocally which of the two descriptions must be preferred.

A last comment concerns the importance of the interaction of VO^{2+} ion and, in general, of vanadium compounds with holo-transferrin. In the course of the years, the different activity of insulin-enhancing VOL_2 compounds was related to the structural features, to the absorption in the gastrointestinal tract, to the biotransformation in the blood serum, and to the interaction with the cell membrane. On the basis of the data in the literature, most of VO^{2+} should be transported in the blood by apo-hTf and monoferric hTf in the specific binding sites as (VO)(apo-hTf) and/or $(VO)_2$(apo-hTf).[13a,c] These conclusions do not explain the significant differences in the insulin-enhancing activity of vanadium compounds, since it is not clear in the literature if the coordination of VO^{2+} ion to hTf is able to yield the "closed" conformation recognized by the hTf receptor. The data reported in this study suggest, instead, that vanadium compounds which form with holo-hTf the ternary species *cis*-VOL_2(holo-hTf)—each one with a specific thermodynamic stability—could be transported inside the cell following the internalization of holo-hTf and this mechanism could be an alternative to the postulated passive diffusion of neutral VOL_2 complexes.[60] In contrast, the mixed complexes formed by apo-hTf, *cis*-VOL_2(apo-hTf), (VO)(apo-hTf)(L), $(VO)_2$(apo-hTf)(L) or $(VO)_2$(apo-hTf)$(L)_2$, cannot be internalized following this pathway because apo-hTf is not recognized by the transferrin receptor. Therefore, the formation of ternary species with holo-hTf, in the presence of iron bound in the specific sites, is a further possible mechanism of transport of insulin-enhancing compounds in the blood toward the target organs and may explain the widespread insulin-enhancing activities exerted by the different VO^{2+} compounds.

AUTHOR INFORMATION

Corresponding Author

*E-mail: garribba@uniss.it.

Notes

The authors declare no competing financial interest.

REFERENCES

(1) MacGillivray, R. T.; Mendez, E.; Shewale, J. G.; Sinha, S. K.; Lineback-Zins, J.; Brew, K. *J. Biol. Chem.* **1983**, *258*, 3543−3553.

(2) Crichton, R. *Iron Metabolism—From Molecular Mechanisms to Clinical Consequences*, 3rd ed.; John Wiley & Sons: Chichester, U.K., 2009.

(3) Sun, H.; Cox, M.; Li, H.; Sadler, P. *Struct. Bonding (Berlin, Ger.)* **1997**, *88*, 71−102.

(4) Sun, H.; Li, H.; Sadler, P. J. *Chem. Rev.* **1999**, *99*, 2817−2842.

(5) Gomme, P. T.; McCann, K. B.; Bertolini, J. *Drug Discov. Today* **2005**, *10*, 267−273.

(6) Andersen, B. F.; Baker, H. M.; Morris, G. E.; Rumball, S. V.; Baker, E. N. *Nature* **1990**, *344*, 784−787.

(7) Eckenroth, B. E.; Steere, A. N.; Chasteen, N. D.; Everse, S. J.; Mason, A. B. *Proc. Natl. Acad. Sci. U. S. A.* **2011**, *108*, 13089−13094.

(8) Rehder, D. *Bioinorganic Vanadium Chemistry*; John Wiley & Sons: Chichester, U.K., 2008.

(9) Costa Pessoa, J.; Tomaz, I. *Curr. Med. Chem.* **2010**, *17*, 3701−3738.

(10) De Cremer, K.; Van Hulle, M.; Chéry, C.; Cornelis, R.; Strijckmans, K.; Dams, R.; Lameire, N.; Vanholder, R. *J. Biol. Inorg. Chem.* **2002**, *7*, 884−890.

(11) Nagaoka, M. H.; Akiyama, H.; Maitani, T. *Analyst* **2004**, *129*, 51−54.

(12) Liboiron, B. D.; Thompson, K. H.; Hanson, G. R.; Lam, E.; Aebischer, N.; Orvig, C. *J. Am. Chem. Soc.* **2005**, *127*, 5104−5115.

(13) (a) Kiss, T.; Jakusch, T.; Hollender, D.; Dörnyei, Á.; Enyedy, É. A.; Costa Pessoa, J.; Sakurai, H.; Sanz-Medel, A. *Coord. Chem. Rev.* **2008**, *252*, 1153−1162. (b) Jakusch, T.; Hollender, D.; Enyedy, E. A.; Gonzalez, C. S.; Montes-Bayon, M.; Sanz-Medel, A.; Costa Pessoa, J.; Tomaz, I.; Kiss, T. *Dalton Trans.* **2009**, 2428−2437. (c) Jakusch, T.; Costa Pessoa, J.; Kiss, T. *Coord. Chem. Rev.* **2011**, *255*, 2218−2226.

(14) (a) Sanna, D.; Garribba, E.; Micera, G. *J. Inorg. Biochem.* **2009**, *103*, 648−655. (b) Sanna, D.; Micera, G.; Garribba, E. *Inorg. Chem.* **2009**, *48*, 5747−5757. (c) Sanna, D.; Micera, G.; Garribba, E. *Inorg. Chem.* **2010**, *49*, 174−187. (d) Sanna, D.; Buglyó, P.; Micera, G.; Garribba, E. *J. Biol. Inorg. Chem.* **2010**, *15*, 825−839. (e) Sanna, D.; Micera, G.; Garribba, E. *Inorg. Chem.* **2011**, *50*, 3717−3728. (f) Sanna, D.; Biro, L.; Buglyo, P.; Micera, G.; Garribba, E. *Metallomics* **2012**, *4*, 33−36. (g) Sanna, D.; Bíró, L.; Buglyó, P.; Micera, G.; Garribba, E. *J. Inorg. Biochem.* **2012**, *115*, 87−99.

(15) (a) Nielsen, F. H. *Vanadium Compounds: Chemistry, Biochemistry and Therapeutic Applications*; American Chemical Society: Washington, DC, USA, 1998; Vol. *711*, pp 297−307. (b) Kustin, K.; Robinson, W. E. In *Metal Ions in Biolical Systems*; Sigel, H., Sigel, A., Eds.; Marcel Dekker: New York, 1995; Vol. *31*, pp 511−542.

(16) Chasteen, D. N. *Coord. Chem. Rev.* **1977**, *22*, 1−36.

(17) Chasteen, D. N. In *Biological Magnetic Resonance*; Berliner, L. J. J., Reuben, J., Eds.; Plenum Press: New York, 1981; Vol. 3, pp 53−119.

(18) Kiss, T.; Jakusch, T.; Bouhsina, S.; Sakurai, H.; Enyedy, É. A. *Eur. J. Inorg. Chem.* **2006**, 3607−3613.

(19) Campbell, R. F.; Chasteen, N. D. *J. Biol. Chem.* **1977**, *252*, 5996−6001.
(20) Smith, C. A.; Ainscough, E. W.; Brodie, A. M. *J. Chem. Soc., Dalton Trans.* **1995**, 1121−1126.
(21) Justino, G. C.; Garribba, E.; Costa Pessoa, J. *J. Biol. Inorg. Chem.* **2013**, *18*, 803−813.
(22) Mason, A. B.; Halbrooks, P. J.; James, N. G.; Connolly, S. A.; Larouche, J. R.; Smith, V. C.; MacGillivray, R. T. A.; Chasteen, N. D. *Biochemistry* **2005**, *44*, 8013−8021.
(23) Sadler, P. J.; Li, H.; Sun, H. *Coord. Chem. Rev.* **1999**, *185*−*186*, 689−709.
(24) Qian, Z. M.; Li, H.; Sun, H.; Ho, K. *Pharmacol. Rev.* **2002**, *54*, 561−587.
(25) Piccioli, F.; Sabatini, S.; Messori, L.; Orioli, P.; Hartinger, C. G.; Keppler, B. K. *J. Inorg. Biochem.* **2004**, *98*, 1135−1142.
(26) Timerbaev, A. R.; Hartinger, C. G.; Aleksenko, S. S.; Keppler, B. K. *Chem. Rev.* **2006**, *106*, 2224−2248.
(27) (a) Thompson, K. H.; Orvig, C. *Coord. Chem. Rev.* **2001**, *219*−*221*, 1033−1053. (b) Shechter, Y.; Goldwaser, I.; Mironchik, M.; Fridkin, M.; Gefel, D. *Coord. Chem. Rev.* **2003**, *237*, 3−11. (c) Thompson, K. H.; Orvig, C. *J. Inorg. Biochem.* **2006**, *100*, 1925−1935. (d) Sakurai, H.; Yoshikawa, Y.; Yasui, H. *Chem. Soc. Rev.* **2008**, *37*, 2383−2392.
(28) (a) Thompson, K. H.; McNeill, J. H.; Orvig, C. *Chem. Rev.* **1999**, *99*, 2561−2572. (b) Thompson, K. H.; Orvig, C. *J. Chem. Soc., Dalton Trans.* **2000**, 2885−2892. (c) Thompson, K. H.; Liboiron, B. D.; Hanson, G. R.; Orvig, C. *Medicinal Inorganic Chemistry*; American Chemical Society: Washington, DC, USA, 2005; Vol. *903*, pp 384−399.
(29) Thompson, K. H.; Lichter, J.; LeBel, C.; Scaife, M. C.; McNeill, J. H.; Orvig, C. *J. Inorg. Biochem.* **2009**, *103*, 554−558.
(30) Sanna, D.; Ugone, V.; Micera, G.; Garribba, E. *Dalton Trans.* **2012**, *41*, 7304−7318.
(31) Mehtab, S.; Gonçalves, G.; Roy, S.; Tomaz, A. I.; Santos-Silva, T.; Santos, M. F. A.; Romão, M. J.; Jakusch, T.; Kiss, T.; Costa Pessoa, J. *J. Inorg. Biochem.* **2013**, *121*, 187−195.
(32) Gonçalves, G.; Tomaz, A. I.; Correia, I.; Veiros, L. F.; Castro, M. M. C. A.; Avecilla, F.; Palacio, L.; Maestro, M.; Kiss, T.; Jakusch, T.; Garcia, M. H. V.; Costa Pessoa, J. *Dalton Trans.* **2013**, *42*, 11841−11861.
(33) Correia, I.; Jakusch, T.; Cobbinna, E.; Mehtab, S.; Tomaz, I.; Nagy, N. V.; Rockenbauer, A.; Costa Pessoa, J.; Kiss, T. *Dalton Trans.* **2012**, *41*, 6477−6487.
(34) (a) Kustin, K.; Toppen, D. L. *Inorg. Chem.* **1973**, *12*, 1404−1407. (b) Cantley, L. C.; Ferguson, J. H.; Kustin, K. *J. Am. Chem. Soc.* **1978**, *100*, 5210−5212. (c) Sakurai, H.; Shimomura, S.; Ishizu, K. *Inorg. Chim. Acta* **1981**, *55*, L67−L69. (d) Baran, E. J. *J. Inorg. Biochem.* **2000**, *80*, 1−10. (e) Wilkins, P. C.; Johnson, M. D.; Holder, A. A.; Crans, D. C. *Inorg. Chem.* **2006**, *45*, 1471−1479.
(35) Yasui, H.; Takechi, K.; Sakurai, H. *J. Inorg. Biochem.* **2000**, *78*, 185−196.
(36) Chasteen, N. D.; Grady, J. K.; Holloway, C. E. *Inorg. Chem.* **1986**, *25*, 2754−2760.
(37) Frisch, M. J.; Trucks, G. W.; Schlegel, H. B.; Scuseria, G. E.; Robb, M. A.; Cheeseman, J. R.; Scalmani, G.; Barone, V.; Mennucci, B.; Petersson, G. A.; Nakatsuji, H.; Caricato, M. L., X.; Hratchian, H. P.; Izmaylov, A. F.; Bloino, J.; Zheng, G.; Sonnenberg, J. L.; Hada, M.; Ehara, M.; Toyota, K.; Fukuda, R.; Hasegawa, J.; Ishida, M.; Nakajima, T.; Honda, Y.; Kitao, O.; Nakai, H.; Vreven, T.; Montgomery, J. A., Jr.; Peralta, J. E.; Ogliaro, F.; Bearpark, M.; Heyd, J. J.; Brothers, E.; Kudin, K. N.; Staroverov, V. N.; Keith, T.; Kobayashi, R.; Normand, J.; Raghavachari, K.; Rendell, A.; Burant, J. C.; Iyengar, S. S.; Tomasi, J.; Cossi, M.; Rega, N.; Millam, J. M.; Klene, M.; Knox, J. E.; Cross, J. B.; Bakken, V.; Adamo, C. J., J.; Gomperts, R.; Stratmann, R. E.; Yazyev, O.; Austin, A. J.; Cammi, R.; Pomelli, C.; Ochterski, J. W.; Martin, R. L.; Morokuma, K.; Zakrzewski, V. G.; Voth, G. A.; Salvador, P.; Dannenberg, J. J.; Dapprich, S.; Daniels, A. D.; Farkas, Ö.; Foresman, J. B.; Ortiz, J. V.; Cioslowski, J.; Fox, D. J. *Gaussian 09*, Revision C.01; Gaussian: Wallingford, CT, USA, 2009.
(38) (a) Jeffrey, P. D.; Bewley, M. C.; MacGillivray, R. T. A.; Mason, A. B.; Woodworth, R. C.; Baker, E. N. *Biochemistry* **1998**, *37*, 13978−13986. (b) He, Q.-Y.; Mason, A. B.; Tam, B. M.; MacGillivray, R. T. A.; Woodworth, R. C. *Biochemistry* **1999**, *38*, 9704−9711.
(39) Krishnan, R.; Binkley, J. S.; Seeger, R.; Pople, J. A. *J. Chem. Phys.* **1980**, *72*, 650−654.
(40) (a) Bühl, M.; Kabrede, H. *J. Chem. Theory Comput.* **2006**, *2*, 1282−1290. (b) Bühl, M.; Reimann, C.; Pantazis, D. A.; Bredow, T.; Neese, F. *J. Chem. Theory Comput.* **2008**, *4*, 1449−1459.
(41) Micera, G.; Garribba, E. *Int. J. Quantum Chem.* **2012**, *112*, 2486−2498.
(42) (a) Baker, E. N.; Baker, H. M.; Kidd, R. D. *Biochem. Cell Biol.* **2002**, *80*, 27−34. (b) Baker, E. N.; Baker, H. M. *Biochimie* **2009**, *91*, 3−10. (c) Baker, E. N.; Baker, H. M. *Cell. Mol. Life Sci.* **2005**, *62*, 2531−2539.
(43) Sanna, D.; Pecoraro, V.; Micera, G.; Garribba, E. *J. Biol. Inorg. Chem.* **2012**, *17*, 773−790.
(44) (a) Micera, G.; Garribba, E. *Dalton Trans.* **2009**, 1914−1918. (b) Micera, G.; Pecoraro, V. L.; Garribba, E. *Inorg. Chem.* **2009**, *48*, 5790−5796. (c) Gorelsky, S.; Micera, G.; Garribba, E. *Chem.−Eur. J.* **2010**, *16*, 8167−8180. (d) Micera, G.; Garribba, E. *Eur. J. Inorg. Chem.* **2010**, 4697−4710. (e) Micera, G.; Garribba, E. *J. Comput. Chem.* **2011**, *32*, 2822−2835. (f) Micera, G.; Garribba, E. *Eur. J. Inorg. Chem.* **2011**, 3768−3780. (g) Sanna, D.; Varnágy, K.; Timári, S.; Micera, G.; Garribba, E. *Inorg. Chem.* **2011**, *50*, 10328−10341. (h) Sanna, D.; Buglyó, P.; Bíró, L.; Micera, G.; Garribba, E. *Eur. J. Inorg. Chem.* **2012**, 1079−1092. (i) Pisano, L.; Varnagy, K.; Timári, S.; Hegetschweiler, K.; Micera, G.; Garribba, E. *Inorg. Chem.* **2013**, *52*, 5260−5272. (j) Sanna, D.; Várnagy, K.; Lihi, N.; Micera, G.; Garribba, E. *Inorg. Chem.* **2013**, *52*, 8202−8213.
(45) Neese, F. *ORCA—An ab Initio, DFT and Semiempirical Program Package*, Version 2.9; Max-Planck-Institute for Bioinorganic Chemistry: Mülheim a. d. Ruhr, Germany, 2012.
(46) Guex, N.; Peitsch, M. C. *Electrophoresis* **1997**, *18*, 2714−2723.
(47) White, L. K.; Chasteen, N. D. *J. Phys. Chem.* **1979**, *83*, 279−284.
(48) Aasa, R. *Biochem. Biophys. Res. Commun.* **1972**, *49*, 806−812.
(49) Aisen, P.; Aasa, R.; Malmström, B. G.; Vänngård, T. *J. Biol. Chem.* **1967**, *242*, 2484−2490.
(50) Chasteen, N. D.; Francavilla, J. *J. Phys. Chem.* **1976**, *80*, 867−871.
(51) DeKoch, R. J.; West, D. J.; Cannon, J. C.; Chasteen, N. D. *Biochemistry* **1974**, *13*, 4347−4354.
(52) De Boer, E.; Boon, K.; Wever, R. *Biochemistry* **1988**, *27*, 1629−1635.
(53) Smith, T. S.; Root, C. A.; Kampf, J. W.; Rasmussen, P. G.; Pecoraro, V. L. *J. Am. Chem. Soc.* **2000**, *122*, 767−775.
(54) (a) Wally, J.; Buchanan, S. *BioMetals* **2007**, *20*, 249−262. (b) Mizutani, K.; Toyoda, M.; Mikami, B. *Biochim. Biophys. Acta, Gen. Subj.* **2012**, *1820*, 203−211.
(55) Buglyó, P.; Kiss, E.; Fábián, I.; Kiss, T.; Sanna, D.; Garribba, E.; Micera, G. *Inorg. Chim. Acta* **2000**, *306*, 174−183.
(56) (a) Buglyo, P.; Kiss, T.; Kiss, E.; Sanna, D.; Garribba, E.; Micera, G. *J. Chem. Soc., Dalton Trans.* **2002**, 2275−2282. (b) Rangel, M.; Leite, A.; João Amorim, M.; Garribba, E.; Micera, G.; Lodyga-Chruscinska, E. *Inorg. Chem.* **2006**, *45*, 8086−8097.
(57) Wally, J.; Halbrooks, P. J.; Vonrhein, C.; Rould, M. A.; Everse, S. J.; Mason, A. B.; Buchanan, S. K. *J. Biol. Chem.* **2006**, *281*, 24934−24944.
(58) Noinaj, N.; Easley, N. C.; Oke, M.; Mizuno, N.; Gumbart, J.; Boura, E.; Steere, A. N.; Zak, O.; Aisen, P.; Tajkhorshid, E.; Evans, R. W.; Gorringe, A. R.; Mason, A. B.; Steven, A. C.; Buchanan, S. K. *Nature* **2012**, *483*, 53−58.
(59) (a) Kiss, E.; Petrohán, K.; Sanna, D.; Garribba, E.; Micera, G.; Kiss, T. *Polyhedron* **2000**, *19*, 55−61. (b) Kiss, E.; Garribba, E.; Micera, G.; Kiss, T.; Sakurai, H. *J. Inorg. Biochem.* **2000**, *78*, 97−108.
(60) Yang, X.; Wang, K.; Lu, J.; Crans, D. C. *Coord. Chem. Rev.* **2003**, *237*, 103−111.

NOTE ADDED AFTER ASAP PUBLICATION

This paper was published on the Web on October 3, 2013, with minor text errors throughout the paper. The corrected version was reposted on October 4, 2013.

dx.doi.org/10.1021/ic401716x | *Inorg. Chem.* 2013, 52, 11975−11985